

Figure S1

Figure S1: Cell cycle status at diagnosis and across treatment cycles

(A) Percentage of HSCs in **(i)** S/G₂/M, **(ii)** G₀, **(iii)** G₁ cell cycle phases. **(i-iii)** *Left*: percentage of cells in specified cell cycle phase at C7D1, coloured by clinical outcome at the end of the oral phase. For patients who did not complete 6 cycles, those with progression during the oral phase or soon after stopping treatment were assessed as non-responders (n = 6), and remaining patients were assigned response as per end of cycle 6 IWG assessment (n = 2). *Right*: Percentage of cells in specified cell cycle phase at C7D1 and at the end (C12D28) of the oral phase. Lines indicate paired samples from a single patient, only patients with data at C7 and C12 are shown. *** $P < 0.001$, ** $P < 0.01$, * $P < 0.05$ unpaired (*left*) or paired (*right*) t-test.

(B) Percentage of HPCs in **(i)** S/G₂/M, **(ii)** G₀, **(iii)** G₁ cell cycle phases. **(i-iii)** *Left*: percentage of cells in specified cell cycle phase at C7D1, coloured by clinical outcome at the end of the oral phase. For patients who did not complete 6 cycles, those with progression during the oral phase or soon after stopping treatment were assessed as non-responders (n = 6), and remaining patients were assigned response as per end of cycle 6 IWG assessment (n = 2). *Right*: Percentage of cells in specified cell cycle phase at C7D1 and at the end (C12D28) of the oral phase. Lines indicate paired samples from a single patient, only patients with data at C7 and C12 are shown. *** $P < 0.001$, ** $P < 0.01$, * $P < 0.05$ unpaired (*left*) or paired (*right*) t-test.

(C) Percentage of HSCs in S/G₂/M following 12 treatment cycles, coloured by clinical outcome at C12D28. *** $P < 0.001$, ** $P < 0.01$, * $P < 0.05$ unpaired t-test. **(D-E)** Relationship between cell cycle status and drug incorporation and DNA demethylation during cycle 7 in **(D)** HSCs and **(E)** HPCs. **(D-E)** Percentage of cells actively cycling (S/G₂/M phase) at C7D1 compared to maximum drug incorporation (*left*) and minimum relative DNA methylation (*right*) in peripheral blood during the same cycle. Dashed lines indicate baseline values. Gray dots indicate patients for whom response data is unavailable. r = spearman correlation coefficient.

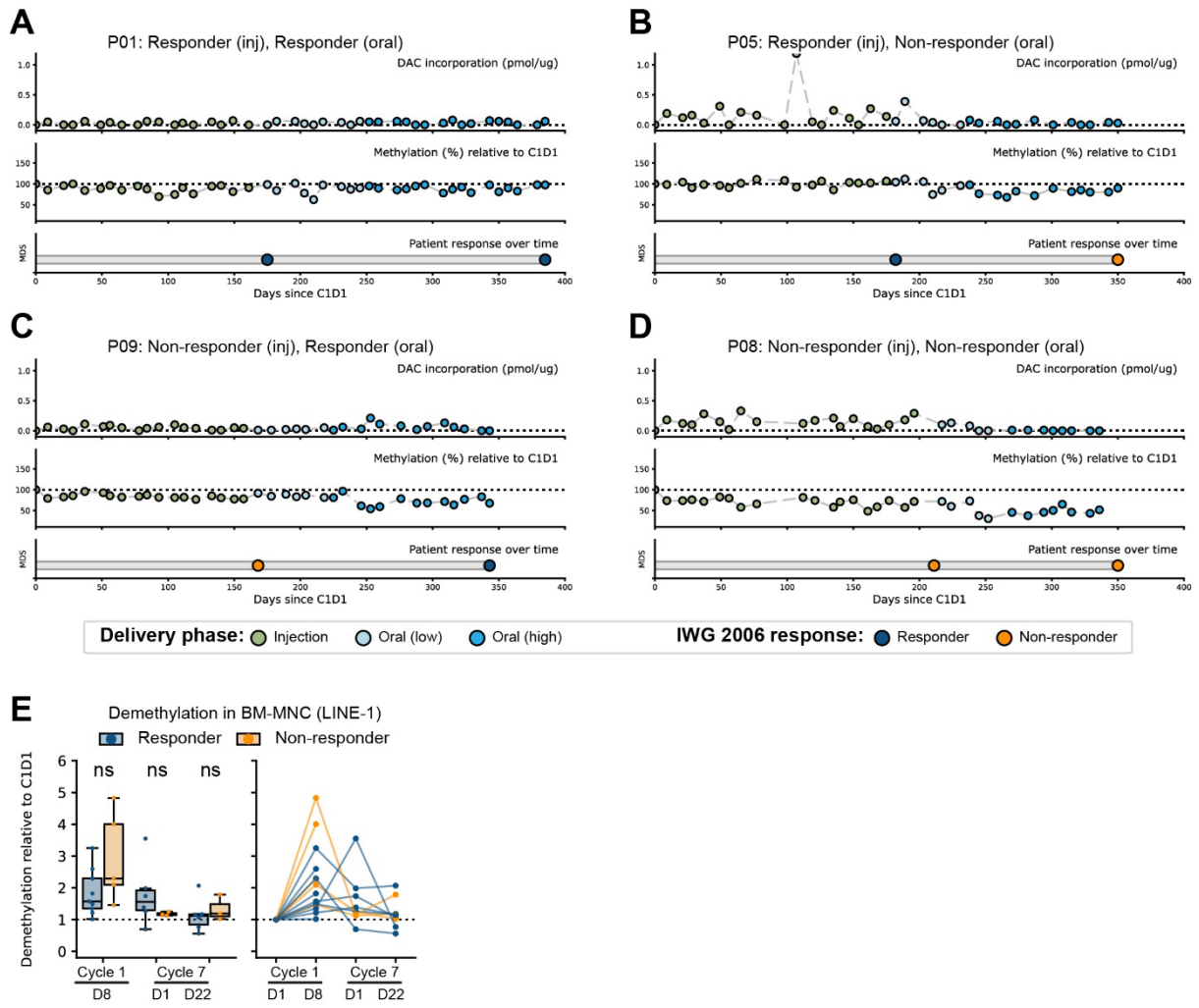


Figure S2

Figure S2: DAC incorporation and relative DNA methylation across treatment phases.

(A-D) Full kinetics of DAC incorporation and relative methylation across the complete treatment timeline for 4 participants with differing patterns of clinical response. Circles show response at IWG assessment or progression timepoints (blue – responder, orange – non-responder). **(E)** Relative DNA demethylation in BM-MNC at C1D8, C7D1, and C7D22 compared to pre-treatment. *Left:* aggregate data at each timepoint. *Right:* Plot showing longitudinal methylation changes in individual patients.

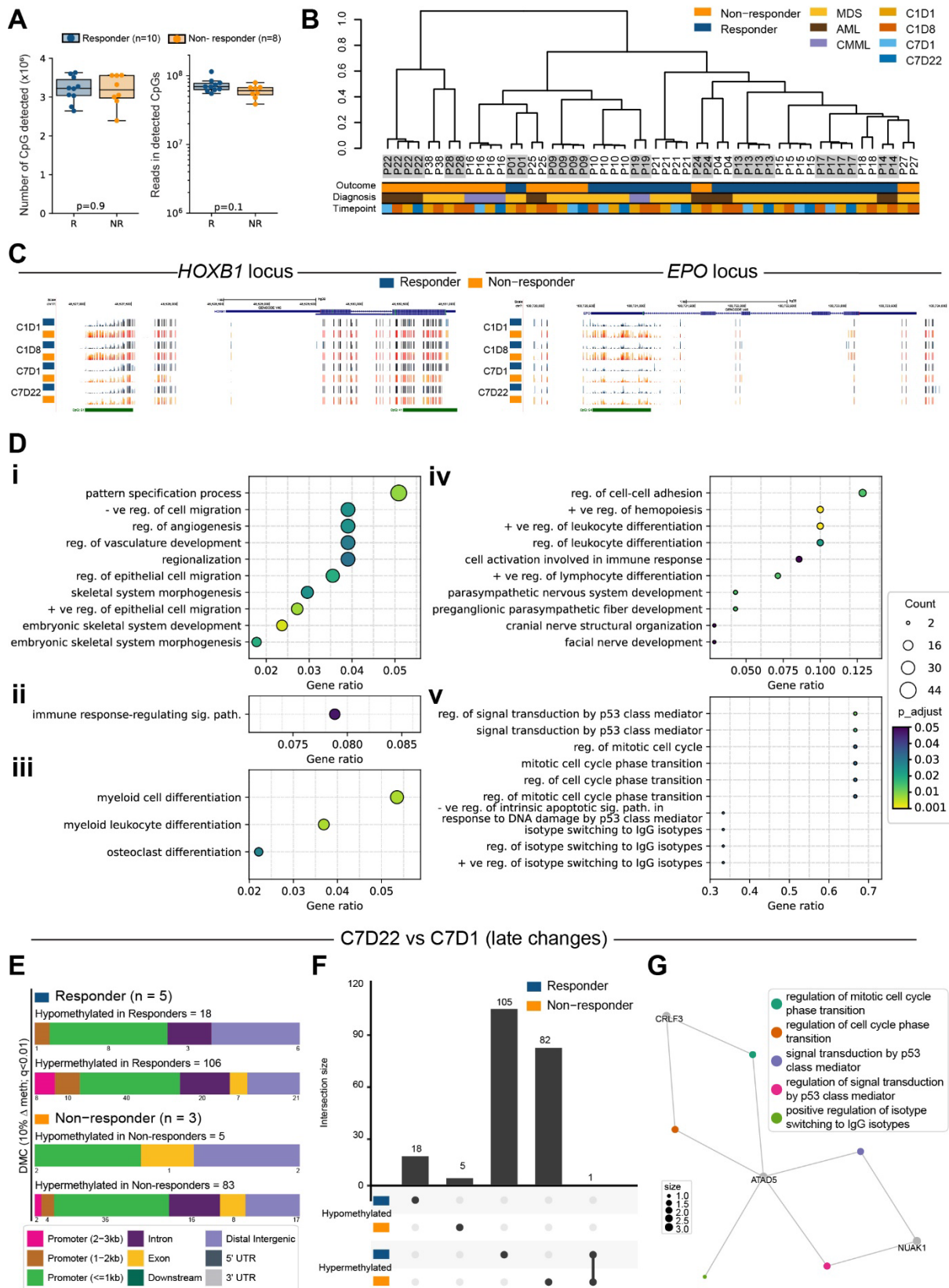


Figure S3

Figure S3: Changes in site-specific methylation over the course of AZA treatment

(A-B) Baseline RRBS data characteristics. **(A)** *Left:* Total number of CpG detected at C1D1, and *Right:* Total number of reads covering detected CpGs at C1D1. **(B)** Hierarchical clustering of all samples based on the most variable CpGs (top 50% based on standard deviation). **(C)** Representative UCSC tracks showing differentially methylated CpGs at the *HOXB1* (chr17:48,526,692-48,531,309 [hg38]) and *EPO* (chr7:100,719,795-100,724,032 [hg38]) loci. Tracks show composite data for each response group at each time point. **(D)** **(i-v)** Gene ontology analysis for genes associated with differentially methylated CpGs. **(i)** Pathways enriched for genes associated with differentially methylated CpGs hypomethylated in responders compared to non-responders at baseline C1D1. **(ii)** Pathways enriched for genes associated with differentially methylated CpGs hypomethylated in both responders and non-responders at C1D8 vs C1D1. **(iii)** Pathways enriched for genes uniquely associated with differentially methylated CpGs hypomethylated in responders at C1D8 vs C1D1. **(iv)** Pathways enriched for genes associated with differentially methylated CpGs hypomethylated in responders at C7D1 vs C1D1. **(v)** Pathways enriched for genes associated with differentially methylated CpGs hypomethylated in responders at C7D22 vs C7D1. **(E-G)** Sustained changes in site-specific methylation. **(E)** Genomic distribution of CpG sites differentially methylated at C7D22 compared to C7D1 in responders. A total of 1144775 CpG were analysed in responders, and 1240814 CpG were analysed in non-responders. **(F)** Upset plot showing overlap of differentially methylated CpG sites between comparison groups. **(G)** Network diagram showing enriched pathways for genes mapping to CpGs which are hypomethylated in responders at C7D22 compared to C7D1 (n = 18 CpGs). Network diagrams were created using clusterProfiler. CpGs were annotated to genes using HiChIP data from healthy human HSPC subsets (Subramanian et al., 2023).

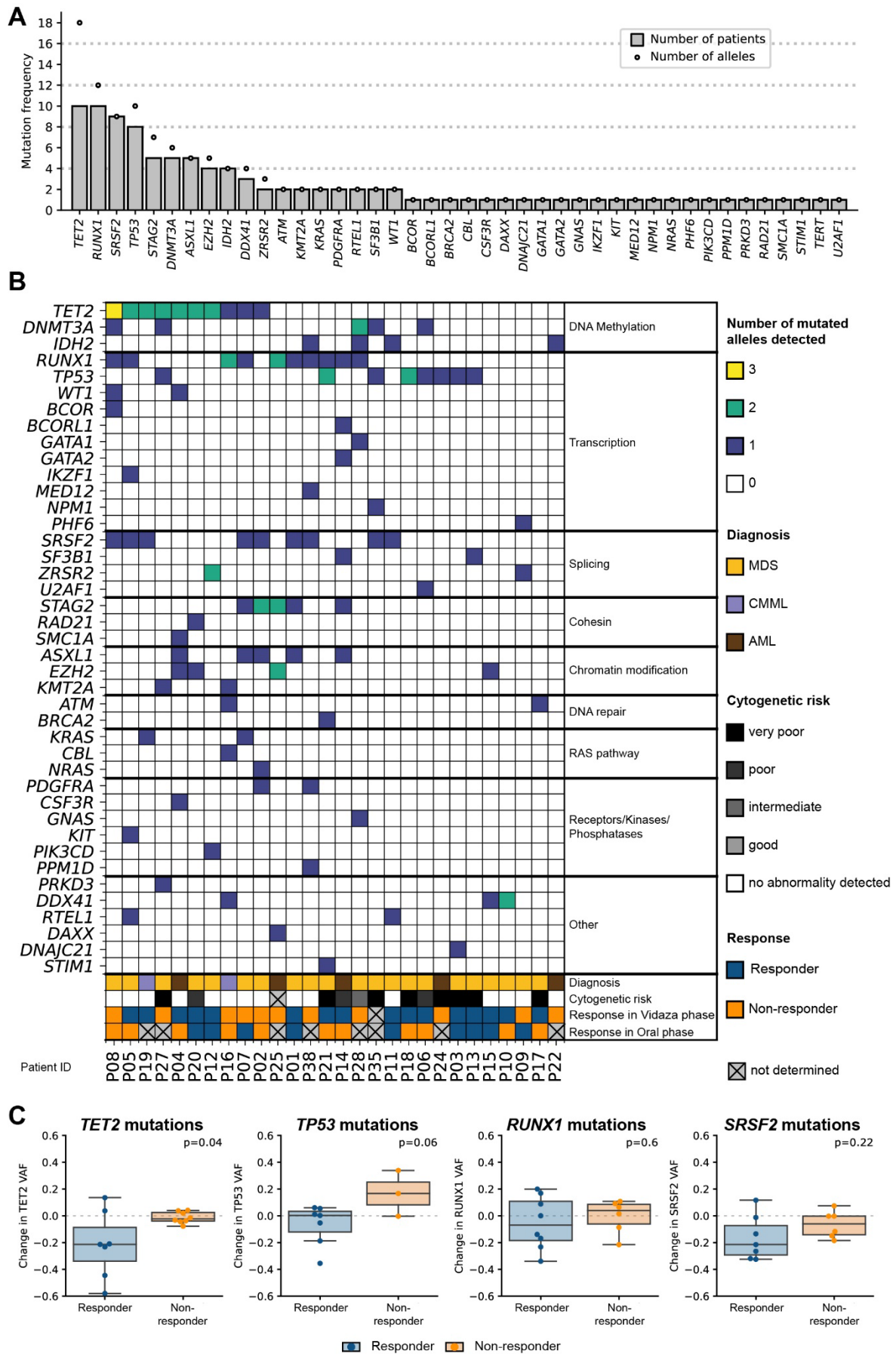


Figure S4

Figure S4: Variations in clonal composition during HMA treatment

(A) Mutation frequency at diagnosis for 28 patients with available data. Grey bars show the number of patients with a mutation detected in the specified gene; open circles indicate the total number of mutated alleles detected in the cohort. **(B)** Overview of mutational profiles in each patient at diagnosis. For each patient, the number of mutated alleles corresponding to each gene is indicated, along with diagnosis, cytogenetic risk score, and response status. Genes are grouped by known function. Cytogenetic risk scores were classified as follows; “no cytogenetic abnormality detected”, “good”: normal karyotype; del(20q); del(5q); del(12p) or double including del(5q), “intermediate”: +8; del(7q); i(17q); +19 or any other single or double independent clone, “poor”: -7; inv(3)/t(3q)/ del(3q); double including -7/del(7q); or complex (3 abnormalities), “very poor”: complex > 3 abnormalities. **(C)** Change in variant allele frequency and patient response status for genes with highest mutation frequency in the cohort. Graphs show combined injection and oral phases, with each data point showing VAF change and corresponding response status. P values shown are for unpaired t-tests.

References

Subramanian, S., Thoms, J.A.I., Huang, Y., Cornejo-Paramo, P., Koch, F.C., Jacquelin, S., Shen, S., Song, E., Joshi, S., Brownlee, C., *et al.* (2023). Genome-wide transcription factor-binding maps reveal cell-specific changes in the regulatory architecture of human HSPCs. *Blood* 142, 1448-1462.